POAC'11
Montréal, Canada

Proceedings of the 21st International Conference on
Port and Ocean Engineering under Arctic Conditions
July 10-14, 2011
Montréal, Canada

POAC11-036

DEVELOPMENT OF A NUMERICAL SIMULATION FOR ROTATING AND SLIDING OF THE ICE FLOES ALONG A SHIP HULL

Junji Sawamura [1], Takashi Tachibana [1]

[1]Department of Naval Architecture and Ocean Engineering, Osaka University, Osaka, JAPAN

ABSTRACT

In this paper, a numerical simulation to calculate the sliding and rotating phases of the ice broken pieces after bending failure of the plate ice when the ship advances in the level ice field is developed. The motions of the broken ice floes are described by the 3DOF rigid body motion in 2-dimentional simulation and 6DOF in 3-dimentional one. A quaternion is adopted to describe the position and rotation instead of using the rotation matrix. The ice pieces and the ship hull are represented by the small contact-spheres which are utilized to detect the contact point between two bodies. The contact force between the broken ice piece and the ship hull is dealt with by the impulsive response. The buoyancy force and the fluid force which is described by the simple formula are considered as the hydrodynamic force acting on the ice pieces. The contribution of the fluid flow induced by the ship advancing is ignored. The simulations are carried out in the both of 2D and 3D conditions. The relationship between the motion of the ice pieces and the ice force in the submerging phase is investigated. The numerical results show that the simulation can describe the mechanism of the rotating and sliding of the ice pieces qualitatively, and has high potential to estimate the submerging component in the ice resistance.

INTRODUCTION

The ice breaking of the ship advancing into a level ice can be represented by two phases: (1) the bending failure of the floating ice sheet; and (2) the rotating-sliding of the broken ice pieces. After the bending failure of the ice sheet, the broken ice piece is rotating and sliding along the ship hull until ice piece is left on the side or behind the ship. The magnitude of the ice load of the ice submerging process is relatively smaller than one of the ice bending failure. However, the submerging component of the ice load has considerable effect on the ice resistance which is defined to be time average force. The ice load of the rotating and sliding are caused by the interaction between the ship hull and ice pieces, whose motion is strongly related with the ship speed, the hull form, the neighbour ice pieces and the surrounding water. The physical phenomenon of the rotating and sliding phase induced by a large amount of the broken ice pieces has not been well understood for the ship design purpose until now.

The model tests with the pre-sawn ice are usually conducted to obtain the ice submerging resistance. The model test is, however, cost inefficiency and cannot be used for the parameter

study of the factors contributing to ice resistance such as a hull form, a ship speed, an ice thickness and so on. Valanto (1992) carried out the 2D model experiments and developed a numerical model of a ship advancing into a floating ice sheet. He focused on transient response of a floating ice sheet at the waterline which is the bending failure and the rotation of the ice broken piece. According experimental results, there is no significant increase in the ice resistance due to ice bending and rotation with speed. Kamarainen (1994) studied the ice submerging component of the ice resistance theoretically. He describes the increase of the ice resistance with the ship speed by the theory called the pressure decrease theory which is related to the pressure decrease between the hull surface and the ice pieces with increasing ship velocity. Puntigliano (1997) also investigated the contribution of the ice sliding on the ice resistance by the model test. The measured data shows that the resistance increases and the vertical force decrease with increasing ship velocity. These researches have uncertainty about the contributions of the rotating and sliding phase on the ice resistance. Konno et al. (2006) predicted the ice clearing resistance with the 3D numerical simulation with the theory of physically based modelling. He investigated the motion of the ice pieces and the contact points between the ship hull and the ice pieces in pre-sawn ice test of the icebreaker model. The simulation still has problems to detect accurate contact points, to defined mechanical properties such as friction and restitution coefficient, and to model the fluid force.

This research presents a numerical simulation to calculate the rotating and sliding of the broken ice pieces after ice bending failure. The numerical simulation is based on the rigid body simulation which is similar approach to Konno et al. (2006). The broken ice pieces and the ship are assumed to be the rigid bodies. The motions of broken ice pieces are described by the rigid body equation (e.g. Baraff, 1997). A quaternion is adopted to describe the position and rotation instead of using the rotation matrix. The sphere contact (e.g. Dimgliana et al., 2000) is applied to the contact detection at a ship hull and ice pieces. Contact force and frictional force at the ship-ice contact surface are considered. The contact response is calculated by the theory based on instantaneous impulse. In addition, the buoyancy force and fluid force of surrounding water are acting on the ice piece. The contributions of the fluid flow around the ship hull and the ice pieces induced by the ship advancing are ignored. In 2D and 3D simulations, the relationship between the motion of the ice pieces and the ice force under the ship waterline are investigated. The dependency of the ship speed on the motions of the ice pieces and the ice force are also investigated in 2D simulations. It is shown that the numerical results can explain the submerging process of the broken ice pieces and have possibility to estimate the ice resistance of the rotating and the sliding components.

NUMERICAL MODEL FOR THE ROTATING AND SLIDING OF ICE PIECES

Rigid body simulation

The broken ice pieces are assumed to be the rigid bodies. The motion of the broken ice piece is described by 3 degrees of freedom (3DOF) rigid body equation in 2D model, and 6DOF in 3D model. The position and the orientation of the broken ice piece are solved by the Newton-Euler formulation based on Newton's second low. The derivative of state vector of $\mathbf{Y}(t)$ is defined as:

$$\frac{d}{dt}\mathbf{Y} = \frac{d}{dt}\begin{bmatrix}\mathbf{x}(t) & \mathbf{R}(t) & \mathbf{P}(t) & \mathbf{L}(t)\end{bmatrix}, \tag{1}$$

where $\mathbf{x}(t)$ is the gravity centre at time = t, $\mathbf{R}(t)$ is rotation matrix, $\mathbf{P}(t)$ is momentum vector, $\mathbf{L}(t)$ is angular momentum vector, respectively. Since the mass m of the body and body-space inertia tensor $\mathbf{I}_{body}$ are constant, we have

$$\dot{\mathbf{P}}(t) = \mathbf{F}(t) = m\dot{\mathbf{v}}(t), \tag{2}$$

$$\dot{\mathbf{L}}(t) = \boldsymbol{\tau}(t) = \mathbf{I}\dot{\boldsymbol{\omega}}(t). \tag{3}$$

$\mathbf{v}(t)$ and $\boldsymbol{\omega}(t)$ are velocity and angular velocity, $\mathbf{F}(t)$ and $\boldsymbol{\tau}(t)$ are the external force vector and the external momentum vectors. Using a conventional rotation matrix $\mathbf{R}(t)$ in Eq. (1) inevitably causes the numerical error. This problem can be alternatively solved by using a quaternion. A quaternion is a type of four elements vector. A quaternion needs only one extra variable being used to describe the three freedoms of the rotation. A quaternion is less numerical error than a rotation matrix. A quaternion is defined as

$$q = s + v_x\mathbf{i} + +v_y\mathbf{j} + +v_z\mathbf{k} \quad \text{where} \quad \mathbf{i}^2 = \mathbf{j}^2 = \mathbf{k}^2 = \mathbf{ijk} = -1, \tag{4}$$

where s, v_x, v_y, v_z are the real numbers. The rotation matrix $\mathbf{R}$(t) is given using a quaternion:

$$\mathbf{R} = \begin{bmatrix} 1-2v_y^2-2v_z^2 & 2v_xv_y-2sv_z & 2v_xv_z+2sv_y \\ 2v_xv_y+2sv_z & 1-2v_x^2-2v_z^2 & 2v_yv_z-2sv_x \\ 2v_xv_z-2sv_y & 2v_yv_z+2sv_x & 1-2v_y^2-2v_y^2 \end{bmatrix}. \tag{5}$$

Contact detection between ship and broken ice pieces

Contact detection is important issue in a numerical simulation which is interacting two or more distinct objects. Increasing the number of distinct objects and complexity of the shape of the individual object cause increase of the calculation time and decrease of the accuracy. In this research, contact spheres are applied for contact detections between the broken ice pieces and the ship hull as shown in Figure 1. The ice pieces and the ship hull are represented by the small contact-spheres. Each small contact sphere on the ship hull and the ice surface is target spheres. The distance between two target spheres only detects the contact point when the distance between two circles equals zero. Contact-sphere is simple algorithm so that it allows us to detect the contact point on complicated two bodies in less computational time. The accuracy of the contact point depends on the radius of the contact sphere.

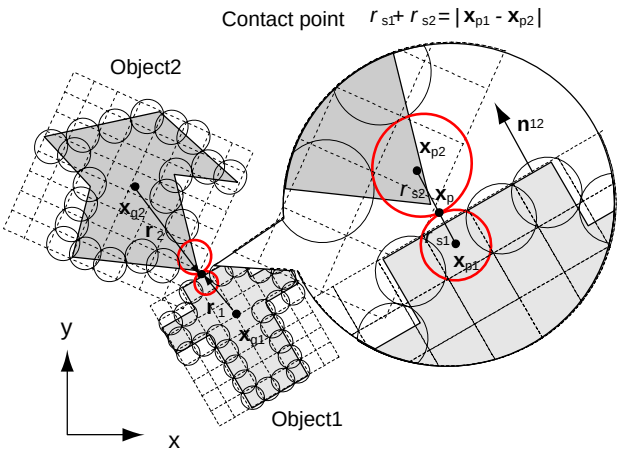

Figure 1. Sphere-contact detection.

Contact response

In this research, the contact response is calculated by the theory based on an instantaneous impulse. The impulse vector **J** at the contact surface is written as follow :

$$\mathbf{J} = j \cdot \mathbf{n}_{12} = \frac{-(1+\varepsilon)v_{ref}}{\frac{1}{m_1} + \frac{1}{m_2} + \mathbf{n}_{12}\left\{\left(\mathbf{I}_1^{-1}(\mathbf{r}_1 \times \mathbf{n}_{12}) \times \mathbf{r}_2\right) + \left(\mathbf{I}_2^{-1}(\mathbf{r}_2 \times \mathbf{n}_{12}) \times \mathbf{r}_1\right)\right\}} \cdot \mathbf{n}_{12}, \tag{6}$$

where $\mathbf{n}_{ij}$ is direction of an impulse force of the object i received from the object j, ε is the coefficient of restitution, v_{ref} is the relative velocity between the contact objects before the application of the impulse, m_i is a mass of the object i, and $\mathbf{I}_i$ is the inertial tensor of the object i, respectively. $\mathbf{r}_i$ is displacement vector representing the displacement from the centre of mass $\mathbf{x}_{gi}$ of the object i to the centre of the contact sphere $\mathbf{x}_{pi}$. The relative velocity at the contact point v_{ref} is calculated by the velocity of centre of mass $\mathbf{v}_{gi}$, the rotational velocity $\boldsymbol{\omega}_{gi}$ before the application of the impulse and contact point displacement $\mathbf{r}_i$:

$$v_{ref} = \mathbf{n}_{12} \cdot \left(\left(\mathbf{v}_{g1} + \boldsymbol{\omega}_{g1} \times \mathbf{r}_1\right) - \left(\mathbf{v}_{g2} + \boldsymbol{\omega}_{g2} \times \mathbf{r}_2\right)\right). \tag{7}$$

Force components

In addition to the contact force, the friction force in tangential direction at the contact surface, the buoyancy force at the gravity centre and the fluid force of surrounding water act on the broken ice piece. The friction force f_s is given by:

$$f_s = -\mu f_n, \tag{8}$$

where f_n is the nominal direction force at the contact surface and μ is friction coefficient. A direction of the friction force is opposite to the relative motion between the ship and the ice at the contact plane. A fluid force from surrounding water acting on the ice piece $\mathbf{F}_w$ is assumed to be following simple formula:

$$\mathbf{F}_w = -\mathrm{C_D} A \frac{1}{2} \rho |\mathbf{v}| \mathbf{v}, \tag{9}$$

where $\mathrm{C_D}$ is a coefficient of drag force, A is a projected area, ρ is a water density and $\mathbf{v}$ is velocity of ice piece. A direction of the fluid force is opposite direction to the motion of the ice piece. In this paper, the contributions of the fluid flow around the ship hull and the ice pieces induced by the ship advancing are ignored. The drag coefficient $\mathrm{C_D}$ is assumed to be 1.0.

NUMERICAL RESULTS AND DISCUSSION

Numerical model

The ship advances straight forward into the broken ice filed as shown in Figure 2. The ship motion is constant with ship velocity 0.2, 0.5, 0.8 and 1.0 m/s in 2D simulations and 0.5m/s in 3D simulation. The motion of the ice pieces are employed by rigid body equations described in previous section. For the initial state of ice pieces, each individual ice piece is separated without interacting with other ice piece, and fixed the initial position before the first contact occurs with the ship hull. A virtual icebreaker model (L×D=10×1.5 in 2D model, L×B×D=10×2×1.8m in 3D model) and a rectangular ice piece (L×D=1×0.4 in 2D model and L×B×D=1×0.8×0.3m in 3D model) as shown in Figure 2 are assumed. The size of the contact sphere is 0.1m radius in both of a ship and an ice for 2D model, and 0.05m in the ice and 0.1m in the ship for 3D model. The different sized and shaped broken ice pieces as shown in actual broken ice can be applied in

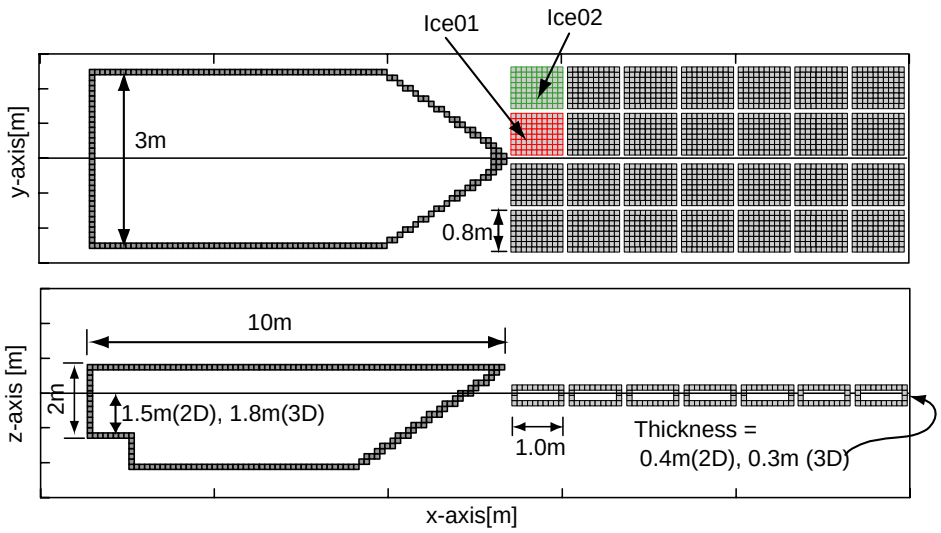

Figure 2. Numerical model.

our simulation. However, only simple broken ice pieces are used as a trial simulation in this research. Friction coefficient for ship-ice contact is 0.1 and 0.3 for ice-ice contact. The coefficient of restitution 0.3 is used both of ship-ice and ice-ice contact. The ice contact force distributions depend on the friction and restriction coefficient. Further research is required to decide appropriate value of the friction and restriction coefficient. The density of ice and water are 900 kg/m^3 and 1000 kg/m^3, respectively. The minimum time step Δt = 0.005s in 2D, and 0.01s in 3D.

Sliding and rotating of ice pieces in 2D model

Figure 3 illustrates the trajectory of the ice pieces in the rotating and sliding process with a ship speed 0.2 m/s. The ice edge contacts with the ship bow and rotates until the ice piece becomes tangent to the ship hull (Figure. 3(a)). The ice is tangentially slid along the ship bow and pushed downward to the ship bottom by the neighbour ice piece (Figure. 3(b) and (c)). The ice is drifting to the astern and hits the propeller domain (Figure. 3(d)). Finally, the ice is left behind the ship (Figure. 3(e) and (f)). These consecutive process are produced one after another (Figure. 3(a)-(f)).

Figure 4 shows the time history of the contact force and the friction force in *x* and *z* direction. In Figure 4(a-1), positive forces show the contact force of the ice rotating and sliding along the ship bow, and negative peak forces show the ice piece hits the propeller domain. In Figure 4(a-2), the force distributions until 60s show the sum of the rotating and sliding force at the bow and bottom hull. The large peak forces observed from 60s mean the ice piece hits the propeller domain. In Figure 4(b), the friction forces become relative smaller than contact force in this simulation, but it might be large contributions on the ice resistance.

Figure 5 illustrates the trajectory of rotating and sliding of ice pieces with different ship velocity of 0.5, 0.8 and 1.0 m/s. Figure 6 shows the time history of the horizontal ice force and vertical one. The different distributions of the ice pieces along the bottom hull in different ship speed are observed in Figure 5. The ice force in both of x and z directions increase with increasing of the ship speed.

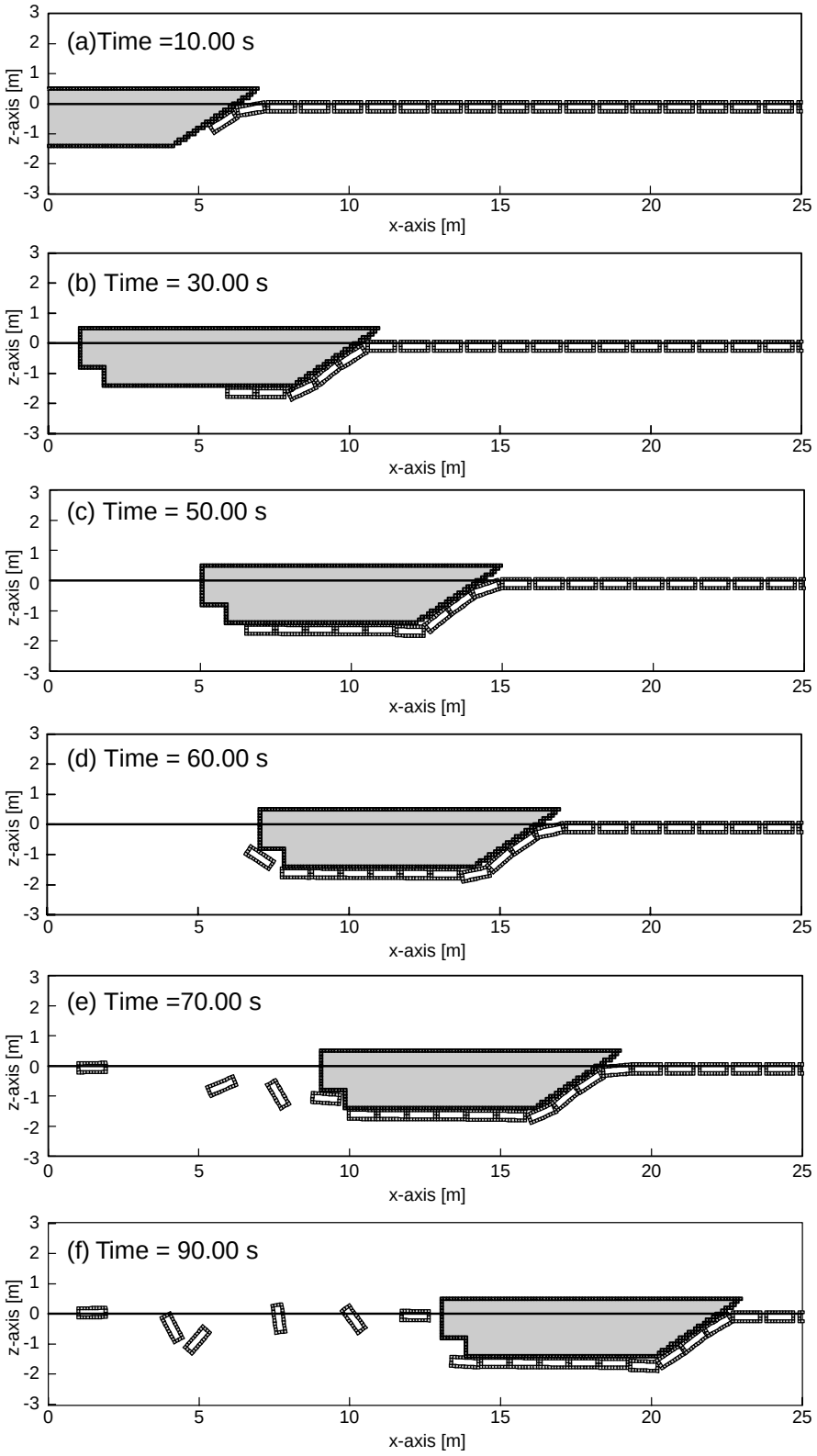

Figure 3. Ice rotating and sliding process in 2D model with ship speed = 0.2 m/s.

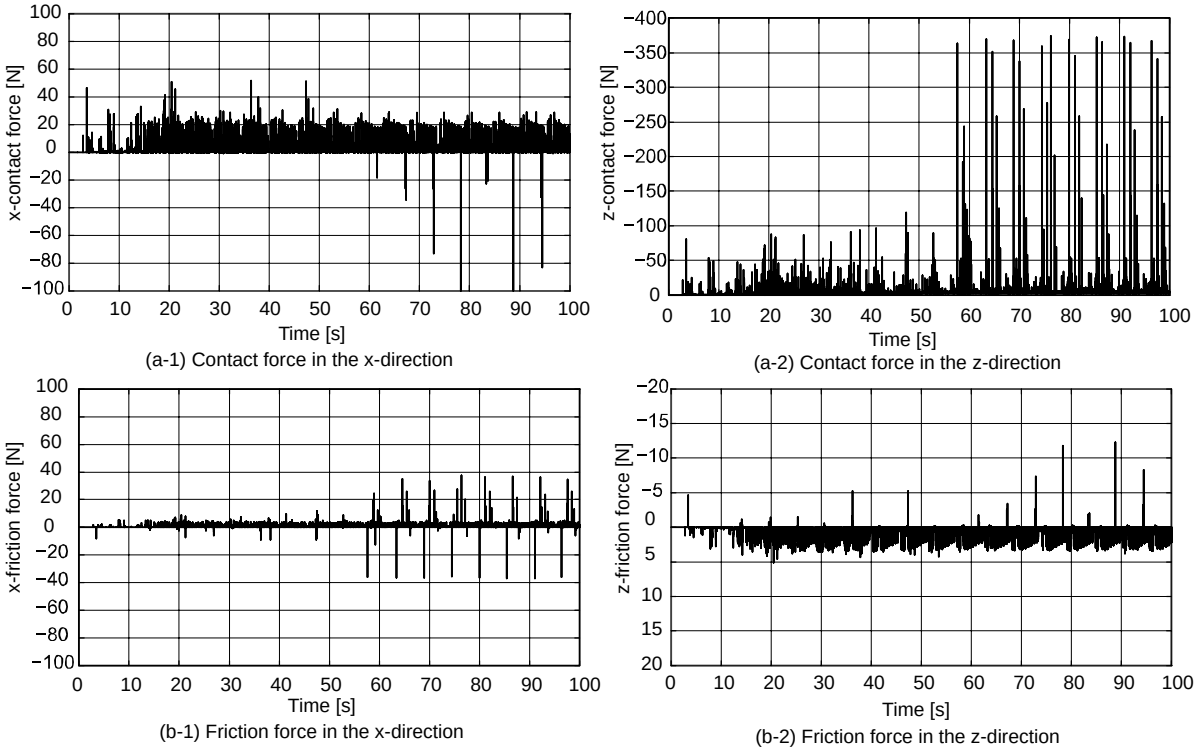

Figure 4. Time history of the contact and friction force in the ice rotating and sliding phase (Ship speed =0.2m/s).

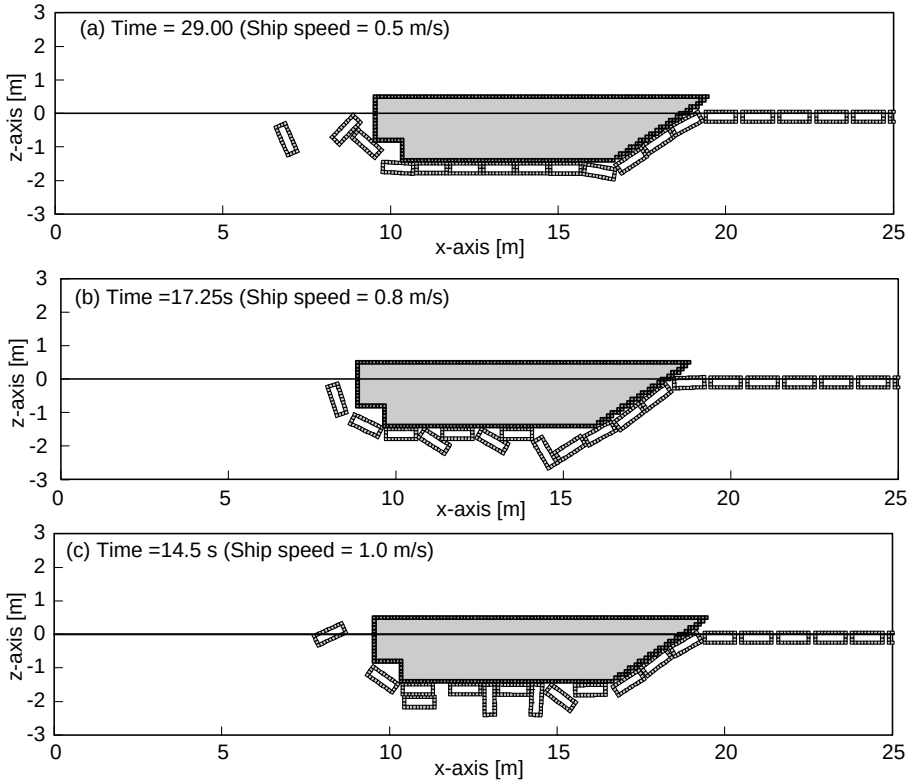

Figure 5. Ice rotating and sliding with different ship speed = 0.5, 0.8 and 1.0 m/s.

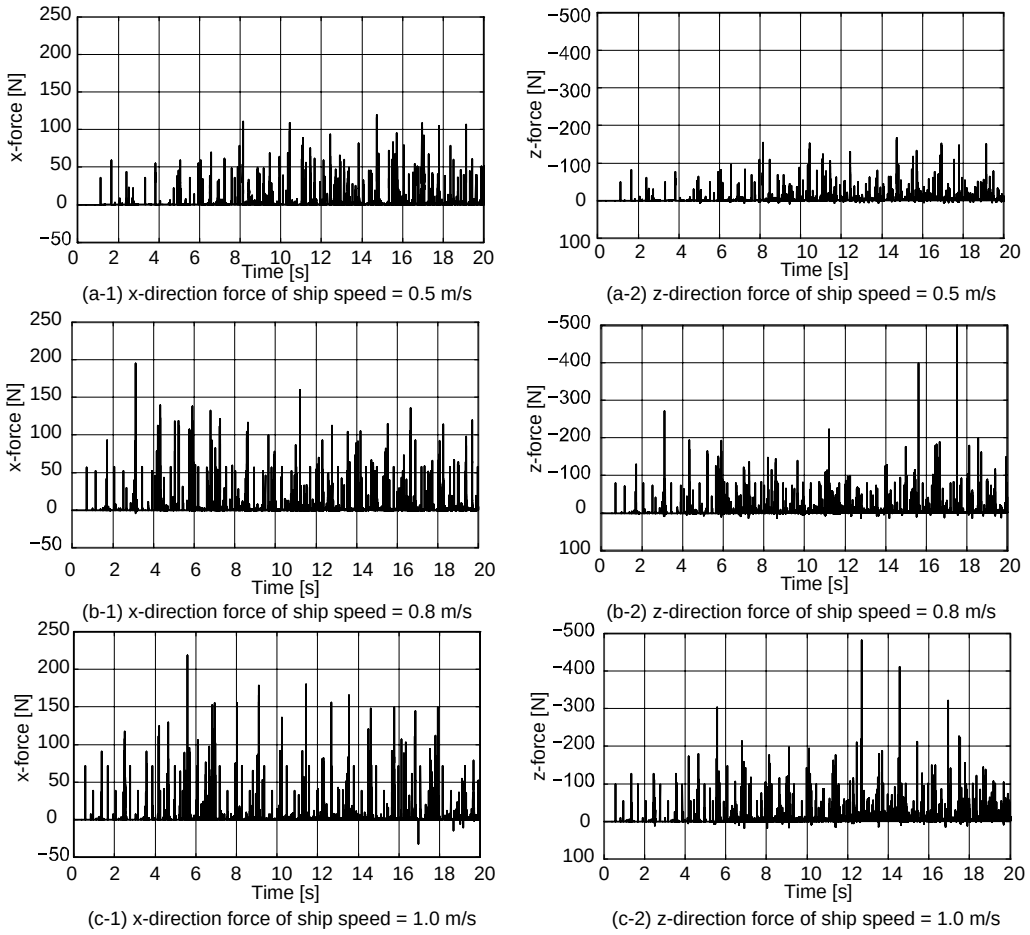

Figure 6. Time history of the contact force with different ship speed = 0.5, 0.8 and 1.0 m/s.

Sliding and rotating of ice pieces in 3D model

Figure 7 illustrates the ice rotating and sliding process in top view (x-y plane), front view (y-z plane) and side view (x-z plane). The ship mainly removes ice pieces to the ship side hull. The ice pieces at the ship centre are pushed down to the bottom hull, and finally left far from the ship side. The ice pieces contacted with the ship shoulder are rotated to the side hull and kept between the ice piece and the ship side hull.

Figure 8 shows the contact force of the centre (ice01 in Figure 2) and side ice piece (ice02 in Figure 2) in x, y and z directions. In Figure 8(a), the ice forces related to the contacts with the ship bow are observed in both of the centre and the side ice. In Figure 8(b), the ice forces related to only shoulder contact of side ice (ice02) are observed. In Figure 8(c), two kind force distributions are observed for centre ice (ice01). The former forces from 0s to 5s are generated by the ice rotating and sliding along the ship bow. Second forces from 10s to 15s are concerned with the bottom contact of the ship. After 15s, the centre ice (ice01) is pushed out to side hull. On the other hand, the side ice (ice02) contacts with ship bow around 5s when ice forces are observed in x and z direction. The side ice is rotated, and contact with the ship shoulder when ice forces occurs in y-direction. Finally, the side ice is kept between the side hull and the ice pieces whose contact does not happen with the ship after 10s. The numerical results in 3D model show the quite different movement of the ice pieces and the force distributions from 2D model. However,

In this paper, the contributions of the fluid flow induced by the ship advancing are ignored in both of 2D and 3D models. We need further investigations about the water flow around the ship hull.

CONCLUSION

This research presents the numerical model which can calculate the rotating and sliding phase in the ice breaking process in 2D and 3D model. We observed the relationship between the motion of the ice piece and the ice force distribution. The numerical results show the presented model can describe the sequence of rotating and sliding of the ice pieces qualitatively. The presented model needs to be verified by pre-sawn model test or measurement data.

ACKNOWLEDGEMENT

This research was supported by the KAKENHI (22760633) and the Shipbuilders' Association of Japan (SAJ).

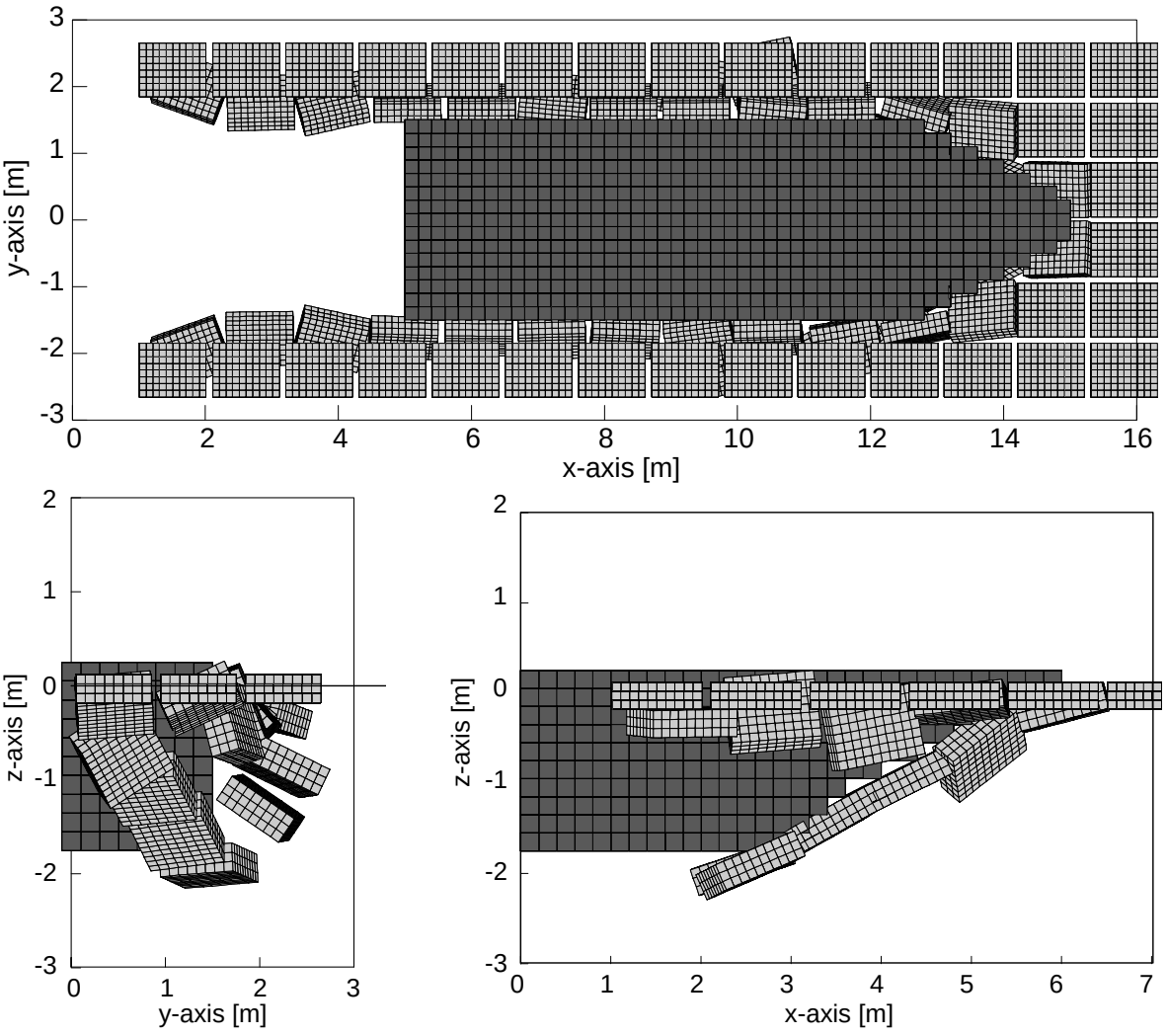

Figure 7. Ship advancing into the broken ice field (Top: x-y, Bottom left: y-z, right: x-z).

REFERENCES

Baraff, D., 1997. Rigid Body Simulation I, II. Siggraph 97 Course notes.

Dimgliana, J. and O'Sullivan, C., 2000. Graceful Degradation of Collision Handling in Physically Based Animation. Computer Graphics Forum, Vol. 19, Issue 3, pp.239-248.

Kamarainen, J., 1994. On the Speed Dependence of the Ice Submerging Resistance in Level Ice. Proc. 4th International Offshore and Polar Engineering Conference, Vol. 2, pp. 578-583.

Konno, A. and Mizuki, T., 2006. Numerical Simulation of Pre-sawn Ice Test of Model Icebreaker Using Physically Based Modelling. Proc. 18th IAHR International Symposium on Ice, Vol. 2, pp. 17-23.

Puntigliano, F. M., 1997. On the Ship Resistance under the Design Waterline in the Continuous Mode of Icebreaking in Level Ice. OMAE, Vol. 4, Arctic/Polar Technology ASME, pp. 73-82.

Valanto, P., 1992. The Icebreaking Problems in Tow Dimensions: Experiments and Theory. Journal of Ship Research, Vol. 36, No.4, pp. 299-316.

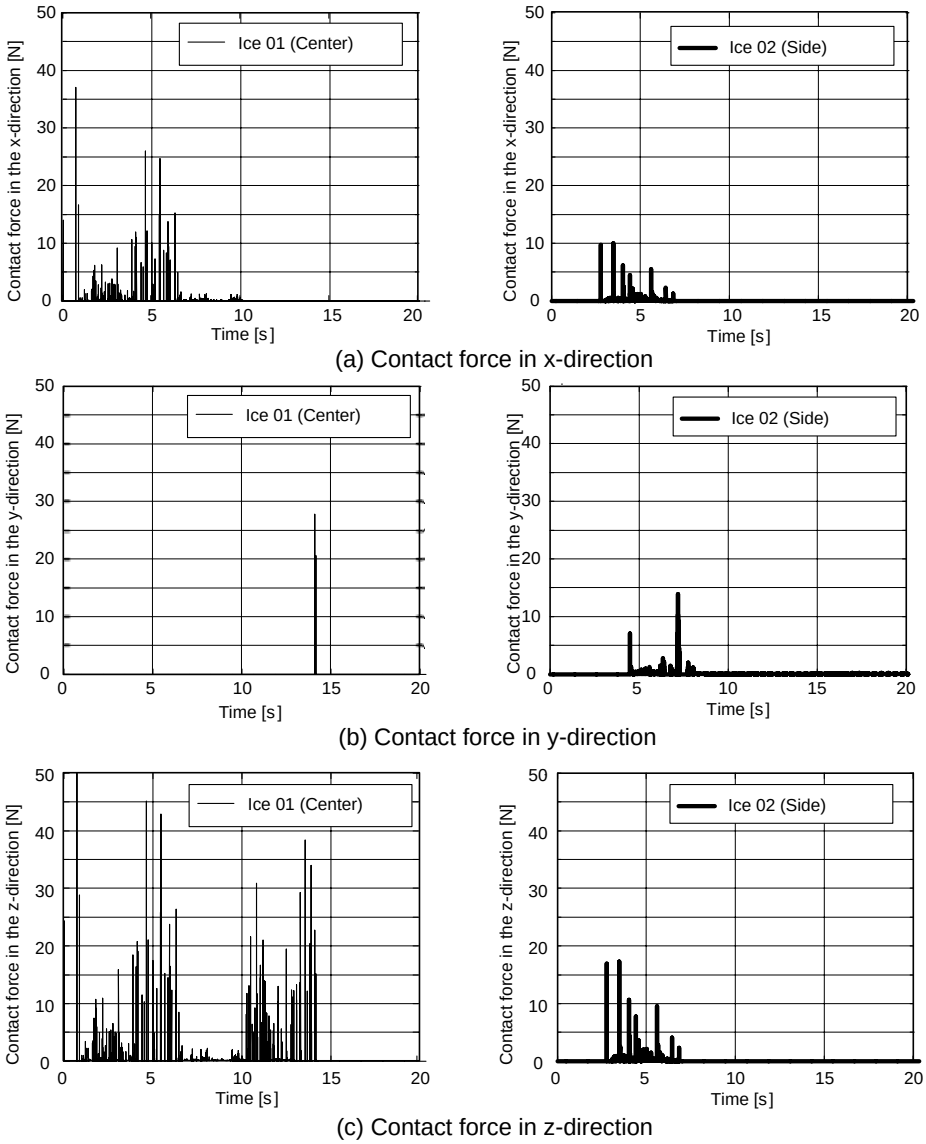

(a) Contact force in x-direction

(b) Contact force in y-direction

(c) Contact force in z-direction

Figure 8. Time history of the contact force of the center ice (ice01) and the side ice (ice02).